Repression of Viral Gene Expression and Replication by the Unfolded Protein Response Effector XBP1u

Florian Hinte[1], Eelco van Anken[2,3], Boaz Tirosh[4], Wolfram Brune[1,*]

1 Heinrich Pette Institute, Leibniz Institute for Experimental Virology, Hamburg, Germany
2 Division of Genetics and Cell Biology, San Raffaele Scientific Institute, Milan, Italy
3 Università Vita-Salute San Raffaele, Milan, Italy
4 Institute for Drug Research, School of Pharmacy, Faculty of Medicine, The Hebrew University, Jerusalem, Israel
* Corresponding author. Phone: +49 40 48051351; Email: wolfram.brune@leibniz-hpi.de

Running title: Cytomegalovirus repression by XBP1u

Word count
Abstract: 165
Text: 4969

Abstract

The unfolded protein response (UPR) is a cellular homeostatic circuit that regulates protein synthesis and processing in the ER by activating three ER-to-nucleus signaling pathways. One of these pathways is triggered by the inositol-requiring enzyme 1 (IRE1), which splices the X-box binding protein 1 (XBP1) mRNA, thereby enabling the expression of the transcription factor XBP1s. Another UPR pathway triggers proteolytic activation of the activating transcription factor 6 (ATF6). Here we show that murine cytomegalovirus (MCMV), a prototypic β-herpesvirus, harnesses the UPR to regulate its own life cycle. MCMV transiently activates the IRE1-XBP1 pathway early post infection in order to relieve repression by XBP1u, the product of the unspliced *Xbp1* mRNA. XBP1u inhibits viral gene expression and replication by blocking the activation of the viral major immediate-early promoter by XBP1s and ATF6. These findings reveal a redundant function of XBP1s and ATF6 as activators of viral gene expression and replication, and an unexpected role of XBP1u as a potent repressor of both XBP1s and ATF6-mediated activation.

Key words: unfolded protein response / transcription factor / XBP1u / ATF6 / cytomegalovirus.

Introduction

The endoplasmic reticulum (ER) is responsible for synthesis, posttranslational modification, and folding of a substantial portion of cellular proteins. When protein synthesis is increased or ER function is compromised, the folding capacity of the ER may get out of balance, leading to an accumulation of unfolded or misfolded proteins in the ER. To alleviate ER stress and restore homeostasis, the cell activates three ER-to-nucleus signaling pathways, collectively called the unfolded protein response (UPR), which lead to a reduced protein synthesis and an increased expression of folding chaperones and ER-associated degradation (ERAD) factors (Walter & Ron, 2011). Subsequently, ER folding capacity increases and terminally misfolded protein species are exported from the ER and targeted for proteasomal degradation (Christianson & Ye, 2014).

In mammalian cells, the UPR comprises three main signaling pathways named after the initiating ER stress sensors: PERK (PKR-like ER kinase), ATF6 (activating transcription factor 6), and IRE1 (inositol-requiring enzyme 1) (Walter & Ron, 2011). Upon activation by ER stress, PERK phosphorylates the translation initiation factor eIF2α, which leads to a massive attenuation of protein synthesis and an immediate reduction of the protein load in the secretory system. However, phosphorylated eIF2α selectively supports the translation of

37 selected cellular proteins such as the transcription factor ATF4, which activates a negative
38 feedback loop resulting in dephosphorylation of eIF2α (Novoa et al, 2001).
39 Upon activation by ER stress, ATF6 travels to the Golgi, where it undergoes
40 intramembrane proteolysis. This process liberates its cytosolic N-terminus, the basic leucine
41 zipper (bZIP) transcription factor ATF6(N), and enables it to travel to the nucleus, where it
42 activates the transcription of chaperone genes as well as of the gene encoding XBP1 (Lee et
43 al, 2002).
44 The third sensor, IRE1, is an ER transmembrane protein kinase that oligomerizes
45 upon accumulation of unfolded proteins in the ER lumen. Oligomerization and auto-
46 transphosphorylation activates the RNase function of IRE1, which mediates an
47 unconventional splicing of the XBP1 mRNA in the cytosol (Calfon et al, 2002; Lee et al, 2002;
48 Yoshida et al, 2001). Removal of the 26-nt intron from the XBP1 mRNA leads to a frame shift
49 and expression of transcription factor XBP1s, comprising an N-terminal basic leucine zipper
50 (bZIP) domain followed by a C-terminal transcription activation domain. In contrast, the
51 unspliced XBP1 mRNA encodes XBP1u, which lacks the transcription activation domain but
52 contains a hydrophobic patch in the C-terminal part. XBP1u is rapidly degraded and has a
53 short half-life (Tirosh et al, 2006). It can interact with XBP1s and ATF6(N) and target them for
54 proteasomal degradation. Therefore, XBP1u is thought acts as a negative regulator involved
55 in fine-tuning the UPR (Tirosh et al, 2006; Yoshida et al, 2006; Yoshida et al, 2009).
56 Moreover, XBP1u affects autophagy by interacting with transcription factor FOXO1 (Zhao et
57 al, 2013). Apart from mediating XBP1 mRNA splicing, IRE1 can also cleave ER-associated
58 mRNA molecules that contain a specific recognition motif (Moore & Hollien, 2015). This
59 process, which leads to mRNA degradation, is called regulated IRE1-dependent mRNA
60 decay (RIDD). However, the importance of RIDD in different cellular processes such as lipid
61 metabolism, antigen presentation, and apoptosis remains incompletely understood (Maurel
62 et al, 2014).
63 During viral replication large quantities of viral proteins must be synthesized. Folding,
64 maturation, and posttranslational modification of secreted and transmembrane proteins take
65 place in the ER and require a plethora of chaperones, foldases, and glycosylating enzymes.
66 While properly folded proteins are transported to the Golgi, unfolded or misfolded proteins
67 are retained in the ER and exported to the cytosol for proteasomal degradation via the ER-
68 associated protein degradation (ERAD) pathway (Smith et al, 2011). However, the high
69 levels of viral envelope glycoproteins that are being synthesized particularly during the late
70 phase of the viral life cycle can overwhelm the folding and processing capacity of the ER and
71 cause accumulation of unfolded and misfolded proteins in the ER (Zhang & Wang, 2012).
72 Cytomegaloviruses (CMVs) are prototypic members of the β subfamily of the
73 *Herpesviridae*. Their large double-stranded DNA genomes contain at least 165 protein-

74 coding ORFs (Dolan et al, 2004) end encode an even larger number of polypeptides (Stern-
75 Ginossar et al, 2012). Through millions of years of co-evolution with their respective hosts,
76 the CMVs have acquired the ability to moderate immune recognition and modulate cellular
77 stress responses to their own benefit (Alwine, 2008; Mocarski, 2002). Considering the
78 important role of the UPR in controlling cell fitness, it is hardly surprising that the CMVs have
79 evolved means to modify the UPR. For instance, human and murine CMV (HCMV and
80 MCMV) induce PERK activation, but limit eIF2α phosphorylation. By doing this the CMVs
81 prevent a global protein synthesis shutoff but allow eIF2α phosphorylation-dependent
82 activation of transcription factor ATF4 (Isler et al, 2005; Qian et al, 2012). The CMVs also
83 increase expression of the ER chaperone BiP to facilitate protein folding and virion assembly
84 (Buchkovich et al, 2008; Buchkovich et al, 2010; Qian et al, 2012), and HCMV uses PERK to
85 induce lipogenesis by activating the cleavage of sterol regulatory element binding protein 1
86 (Yu et al, 2013). We have previously shown that both, MCMV and HCMV, downregulate
87 IRE1 levels and inhibit IRE1 signaling at late times post infection. This downregulation is
88 mediated by the viral proteins M50 and UL50, respectively (Stahl et al, 2013). However, a
89 real-time transcriptional profiling study has revealed that cellular ER stress response
90 transcripts are upregulated as early 5-6 hours after MCMV infection (Marcinowski et al,
91 2012).
92 Here we show that MCMV transiently activates the IRE1-XBP1 pathway at early times
93 postinfection in order to relieve repression of viral gene expression and replication by XBP1u.
94 When IRE1-mediated XBP1 mRNA splicing is inhibited, XBP1u blocks the activation of the
95 viral major immediate-early promoter (MIEP) by XBP1s and ATF6(N). Thus, MCMV exploits
96 UPR signaling to boost the activity of its most important promoter. Moreover, these findings
97 reveal a redundant function of XBP1s and ATF6 as activators of viral gene expression and
98 replication, and an unexpected role of XBP1u as a potent repressor of both XBP1s and
99 ATF6-mediated activation.
100

101 ## Results

102 **Early activation of IRE1-XBP1 signaling promotes MCMV replication.**

103 Previous studies have shown that MCMV inhibits IRE1-XBP1 signaling at late times (≥24 h)
104 post infection (Qian et al, 2012; Stahl et al, 2013). However, cellular ER stress response
105 transcripts were shown to be upregulated at 5-6 hours after MCMV infection (Marcinowski et
106 al, 2012), suggesting that UPR signaling is activated at early times post infection. Thus, we
107 decided to analyze whether MCMV activates the IRE1-XPB1 signaling pathway within the
108 first few hours after infection. To do this, we infected mouse embryonic fibroblasts (MEFs)
109 with MCMV and quantified spliced and unspliced XBP1 transcripts by qRT-PCR. We
110 detected a short and transient increase of XBP1 splicing between 5 and 7 hours post

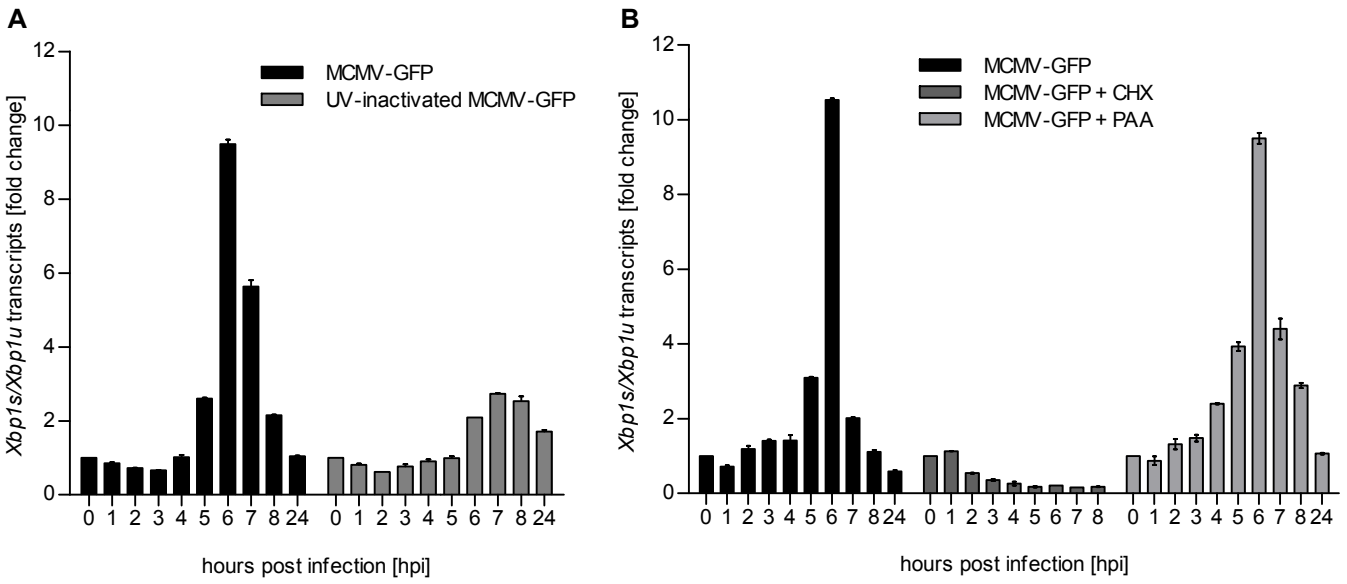

Figure 1.
MCMV induces *Xbp1s* mRNA splicing at early time of infection

A. MEFs were infected with MCMV-GFP or UV-inactivated MCMV-GFP (MOI 4). Cells were harvested at the indicated times, total RNA was extracted, and *Xbp1s* and *Xbp1u* transcripts were quantified by qPCR. Changes in the *Xbp1s/Xbp1u* ratio relative to uninfected cells are plotted as bar diagram (means ±SEM of triplicates).

B. MEFs were infected with MCMV-GFP as described above and treated with vector, CHX (50µg/ml) or PAA (250ng/ml). Changes in the *Xbp1s/Xbp1u* ratio were determined as described above.

111 infection (hpi) (Fig. 1A). This increase was massively reduced when cells were infected with
112 UV-inactivated MCMV (Fig. 1A), suggesting that XBP1 splicing was not caused by viral
113 attachment and entry into cells but required viral gene expression. MCMV-induced XBP1
114 splicing was also suppressed by cycloheximide (CHX, a translation inhibitor), but not by
115 phosphonoacetic acid (PAA), an inhibitor of viral DNA replication and late gene expression
116 (Fig. 1B). These results suggested that the transient activation of the IRE1-XBP1 pathway is
117 caused by viral proteins expressed at immediate-early or early times post infection.
118 To determine whether IRE1 signaling is important for the MCMV life cycle, we used
119 *Ire1*$^{-/-}$ cells expressing IRE1-GFP under tight control of a tetracycline-inducible promoter (Fig.
120 2A) for analyses of viral replication. IRE1-GFP expression was induced with different
121 concentrations of doxycycline, and cells were infected at low or high multiplicity of infection
122 (MOI) for multi-step and single-step growth curves, respectively (Fig. 2B and C). In both
123 types of replication analysis, MCMV replicated to low titers when IRE1 expression was
124 induced with very low or very high doxycycline concentrations. High MCMV titers (~10^6
125 infectious units per ml), comparable to those obtained in wildtype (WT) MEFs, were attained
126 only upon moderate induction of IRE1-GFP with 5 to 10 nM doxycycline (Fig. 2B and C).
127 Thus we concluded that IRE1 is necessary for efficient replication of MCMV, but needs to be
128 carefully regulated as too high expression levels are detrimental for viral replication.
129
130 **IRE1, but not XBP1 or TRAF2, is required for efficient MCMV gene expression and**
131 **replication.**
132 Activated IRE1 can splice *Xbp1* mRNA (Calfon et al, 2002; Lee et al, 2002; Yoshida et al,
133 2001) and can also recruit TRAF2 to activate ASK1 (Urano et al, 2000). To test which IRE1-
134 dependent signaling pathway is required for efficient MCMV replication, we used
135 CRISPR/Cas9-mediated gene editing to generate *Ire1* knockout (ko), *Xbp1* ko, and *Traf2* ko
136 MEFs. For each gene knockout, two independent cell clones were generated with different
137 guide RNAs. The absence of the respective gene products was verified by immunoblot
138 analysis (Fig. 3A). Then the cell clones were used to assess MCMV replication. In *Ire1* ko
139 MEFs, viral replication was reduced by two orders of magnitude as compared to WT MEFs
140 (Fig. 3B), similar to the reduction seen in IRE1-GFP cells without doxycycline induction (Fig.
141 2B). By contrast, MCMV replication was virtually unimpaired in the absence of *Xbp1* (Fig. 3B)
142 or *Traf2* (Fig. 3C). We also analyzed the expression of a viral immediate-early (IE1), an early
143 (M57), and a late protein (gB) at different times post infection. Compared to WT MEFs, the
144 expression of all three proteins was reduced in *Ire1* ko MEFs (Fig. 3D), but not in *Xbp1* or
145 *Traf2* ko MEFs (Fig. 3E and F).
146 Next we tested whether the RNAse activity of IRE1 is required for efficient MCMV
147 replication. To do this, WT IRE1 or an "RNAse-dead" IRE1 K907A mutant (Tirasophon et al,

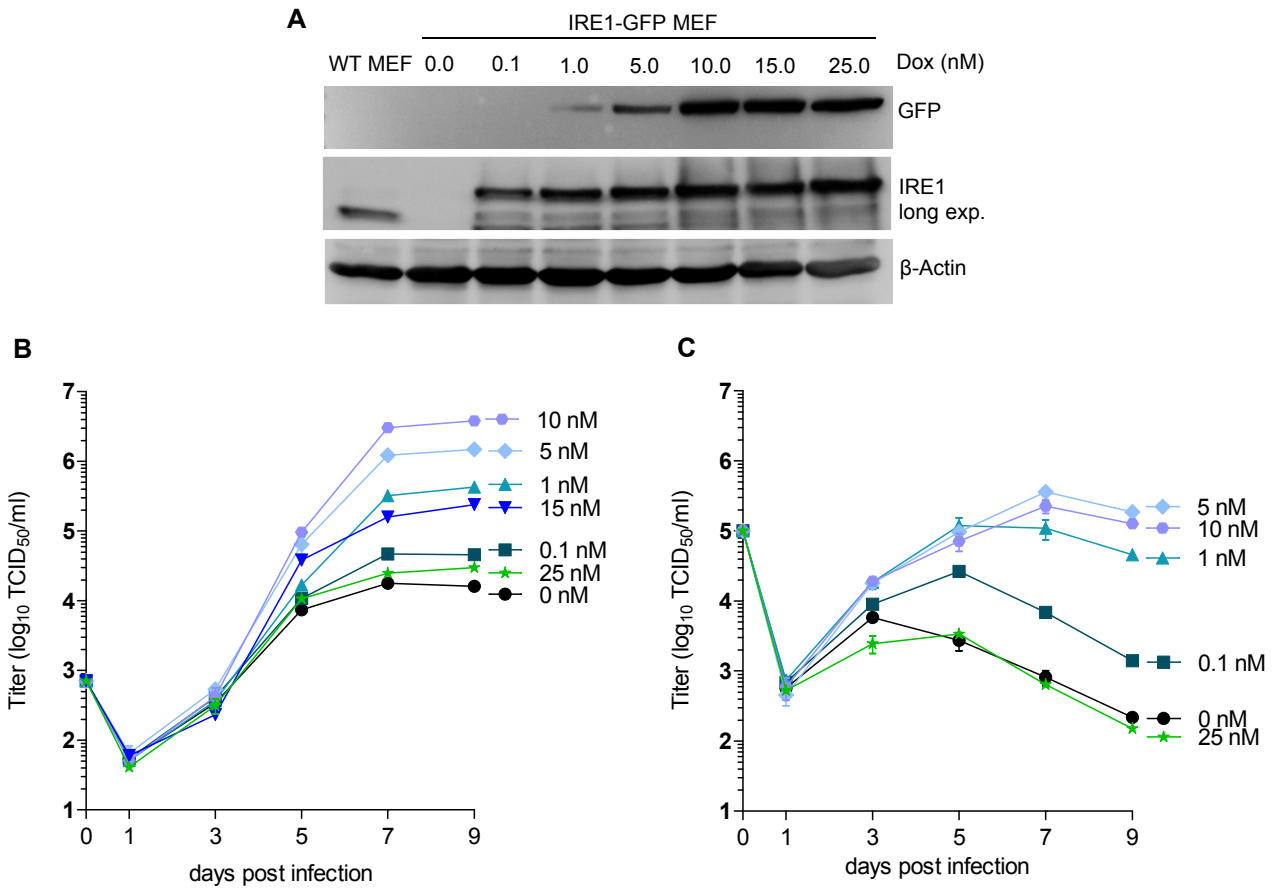

Figure 2.
Moderate IRE1 expression is beneficial for MCMV replication.

A. Immunoblot analysis of *Ire1*$^{-/-}$ MEFs expressing IRE1-GFP in a doxycycline (dox)-inducible manner. Cells were treated with different dox concentrations for 24 h. IRE1-GFP expression was detected with GFP or IRE1-specific antibodies. Endogenous IRE1 levels in WT MEFs were detected only with the IRE1-specific antibody.

B. Multistep MCMV replication kinetics on IRE1-GFP MEFs induced with different dox concentrations. 24 h after induction, cells were infected with MCMV-GFP (MOI 0.1). Virus titers in the supernatants were determined by titration and are shown as means ±SEM of triplicates.

C. Single step MCMV replication kinetics on IRE1-GFP MEFs induced with dox as above and infected with MCMV-GFP (MOI 3).

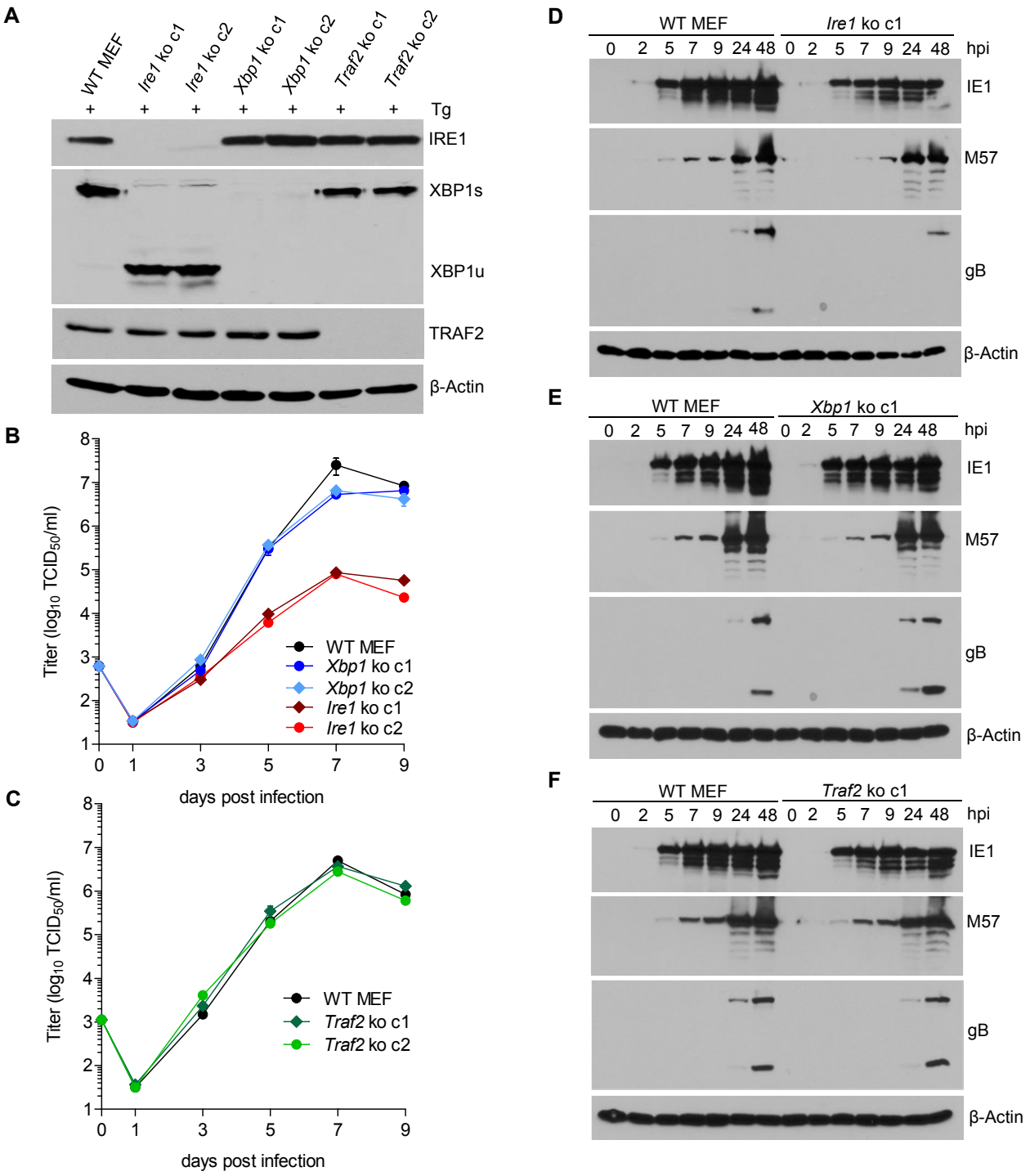

Figure 3.

IRE1, but not XBP1 or TRAF2, is required for efficient MCMV replication and viral protein expression

A. Immunoblot analysis of *Ire1*, *Xbp1* and *Traf2* ko cell lines. Two ko clones were generated for each gene by CRISPR/Cas9 gene editing using different gRNAs. Cells were treated for 4 h with Thapsigargin (Tg) to induce *Xbp1* mRNA splicing and to increase XBP1 expression.

B,C. Multistep MCMV replication kinetics in *Ire1*, *Xbp1* and *Traf2 ko* cells, respectively. Cells were infected with MCMV-GFP (MOI 0.1) Virus titers in the supernatants were determined by titration and are shown as means ±SEM of triplicates.

D-F. Immunoblot analysis of viral protein expression kinetics in *Ire1*, *Xbp1* and *Traf2 ko* cells, respectively. Cells were infected with MCMV-GFP (MOI 3) and harvested at different times post infection. Expression levels of the viral immediate-early 1 (IE1) protein, the major DNA binding protein (M57; an early protein), and glycoprotein B (gB; a late protein) were detected with specific antibodies, β-Actin served as loading control.

148 2000) was expressed in *Ire1* ko MEFs by retroviral transduction. Expression of WT and
149 mutant IRE1 and the ability to splice *Xbp1* was verified by immunoblot analysis (Fig. 4A).
150 While expression of WT IRE1 restored MCMV replication to high titers, expression of IRE1
151 K907A did not increase MCMV titers (Fig. 4B), indicating that the IRE1 RNase activity is
152 necessary for efficient MCMV replication.
153
154 **XBP1u inhibits MCMV replication.**
155 Our observations that the RNase activity of IRE1 is required for efficient MCMV replication,
156 but XBP1 is not, allowed two possible explanations: (i) MCMV replication could benefit from
157 RIDD, another RNase-dependent function of IRE1. However, this possibility is difficult to
158 verify as selective inactivation of RIDD is complicated. (ii) Alternatively, MCMV replication
159 could be inhibited by XBP1u, the product of the unspliced *Xbp1* mRNA, since *Ire1* ko cells
160 differ from other cells in that they express only XBP1u (Fig. 3A). To test the latter option, we
161 used two experimental approaches. First, we knocked out *Ire1* in *Xbp1*-deficient cells (Fig.
162 5A). As shown in figure 5B, MCMV replicated to similar titers in *Xbp1* ko and *Xbp1*/*Ire1*
163 double-knockout (dko) cells, indicating that the loss of IRE1 is not detrimental for MCMV
164 replication when XBP1 is absent. Next, we used retroviral transduction to restore XBP1
165 expression in *Xbp1*$^{-/-}$ cells. The retroviral vectors expressed the WT *Xbp1* transcript (which
166 can be spliced by IRE1), a truncated *Xbp1* transcript encoding only the DNA-binding domain,
167 or an 'unspliceable' *Xbp1* transcript. Upon treatment with thapsigargin, these cells expressed
168 XBP1s, XBP1stop, or XBP1u, respectively (Fig. 5C). Whereas re-introduction of WT XBP1
169 had no detrimental effect, MCMV replication was severely impaired upon expression of the
170 unspliceable *Xbp1* transcript (Fig. 5D), indicating that *Xbp1u* reduces viral replication. A
171 similar inhibitory effect was observed when the truncated XBP1 (XBP1stop) protein was
172 expressed (Fig. 5D).
173
174 **Loss of XBP1 and ATF6 impairs MCMV replication.**
175 XBP1u is thought to function as a negative regulator to XBP1s (Tirosh et al, 2006; Yoshida et
176 al, 2006). However, the inhibition of MCMV replication by XBP1u cannot be explained solely
177 by a repressive effect on XBP1s as a complete loss of XBP1 is not detrimental to MCMV
178 replication in vitro (Fig. 3B) and has only a modest effect on viral replication in vivo (Drori et
179 al, 2014). Thus we hypothesized that XBP1u might impair MCMV replication by repressing
180 the activity of additional transcription factors besides XBP1s. For several reasons ATF6
181 appeared to be a likely target of XBP1u: (i) Like XBP1s, ATF6 is a bZIP transcription factor
182 activated by ER stress (Yoshida et al, 1998); (ii) XBP1s and ATF6 are known to synergize in
183 the activation of numerous ER stress response genes (Lee et al, 2002); and (iii) XBP1u can
184 interact with ATF6 and inhibit its activity (Yoshida et al, 2009). Therefore, we tested whether

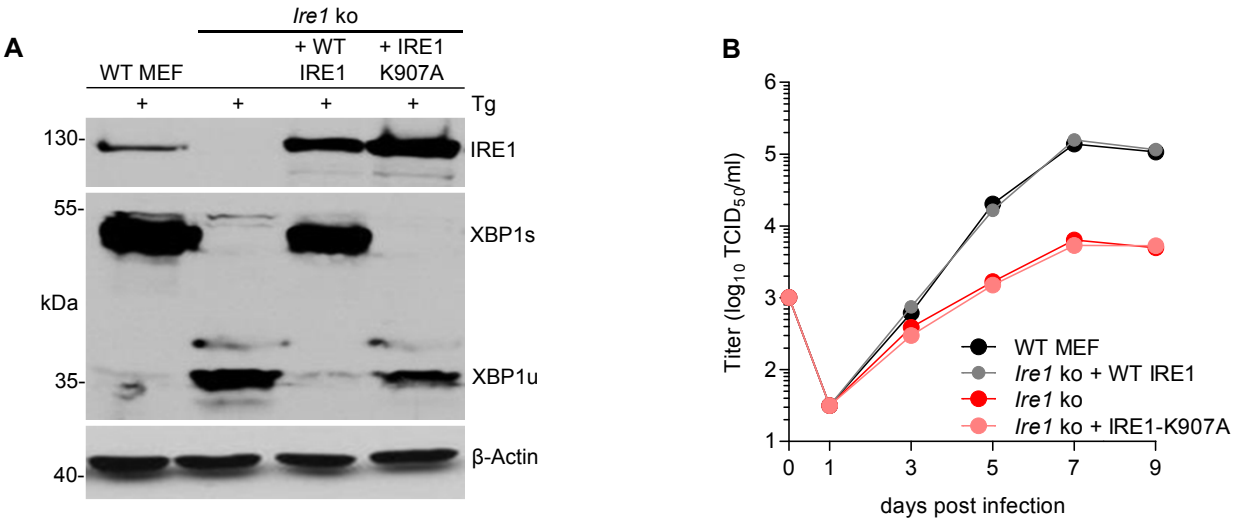

Figure 4.
The RNase function of IRE1 is required for efficient MCMV replication.

A. Immunoblot analysis of *Ire1* ko transduced with retroviral vectors expressing WT IRE1 or IRE1-K907A (RNase-dead). Cells were treated for 4 h with Thapsigargin (Tg) to induce *Xbp1* mRNA splicing and to increase XBP1 expression. IRE1 and XBP1 protein expression was detected by immunoblot.

B. Multistep MCMV replication kinetics in *Ire1 ko* cells complemented with WT IRE1 or IRE1-K907A, respectively. Cells were infected with MCMV-GFP (MOI 0.1). Virus titers in the supernatants were determined by titration and are shown as means ±SEM of triplicates.

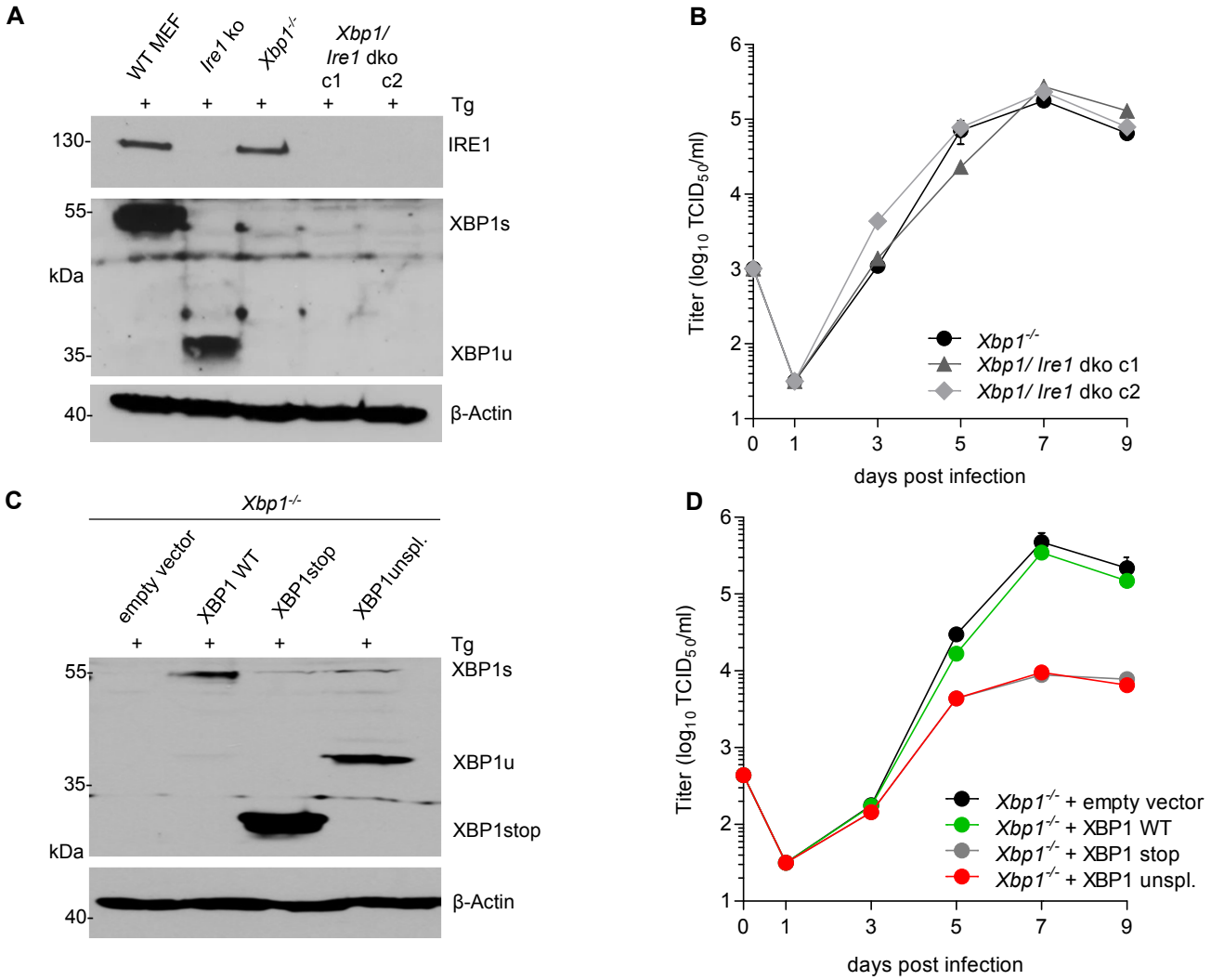

Figure 5.
XBP1u acts as a repressor for MCMV replication.

A. *Xbp1*$^{-/-}$ MEFs were used to knock out *Ire1* by CRISPR/Cas9 gene editing. Two double ko (dko) cell clones were generated with different gRNAs. IRE1 and XBP1 protein expression in the two dko clones and control cells was detected by immunoblot analysis. Cells were treated for 4 h with Thapsigargin (Tg) to induce *Xbp1* mRNA splicing and to increase XBP1 expression.

B. Multistep MCMV replication kinetics in *Xbp1*$^{-/-}$ and *Xbp1/Ire1* dko MEFs. Cells were infected with MCMV-GFP (MOI 0.1) Virus titers in the supernatants were determined by titration and are shown as means ±SEM of triplicates.

C. Immunoblot analysis of *Xbp1*$^{-/-}$ MEF transduced with retroviral vectors expressing a WT (spliceable) *Xbp1* transcript, an unspliceable *Xbp1* transcript, or a truncated (*Xbp1*stop) transcript. Cells were treated with Tg as described in A.

D. Multistep MCMV replication kinetics in cells shown in C. Infection and titration was done as in B.

185 the loss of both, XBP1 and ATF6, was detrimental for MCMV replication. First, we analyzed
186 MEFs from *Atf6*$^{-/-}$ mice and found that MCMV gene expression and replication were not
187 impaired (Fig. 6A and B). When we knocked out *Xbp1* in *Atf6*$^{-/-}$ cells by CRISPR/Cas9 gene
188 editing (Fig. 6C), MCMV replication was substantially reduced in *Atf6*/*Xbp1* dko cells (Fig.
189 6D), suggesting that ATF6 and XBP1s have overlapping or redundant functions and that at
190 least one of them is necessary for efficient MCMV replication.
191
192 **XBP1s and ATF6-mediated activation of the MCMV major immediate-early promoter**
193 **(MIEP) is repressed by XBP1u.**
194 The MCMV MIEP has a key role in viral gene expression as it drives the expression of the
195 viral IE1 and IE3 proteins. IE3 is the major transactivator protein that activates early and late
196 gene expression (Lacaze et al, 2011). Thus we interrogated whether XBP1s and ATF6 can
197 activate the MCMV MIEP. First, we searched for ACGT motifs within the MCMV MIEP. ACGT
198 is a minimal consensus sequence contained within XBP1s and ATF6 binding motifs
199 (Kanemoto et al, 2005; Wang et al, 2000). Five ACGT motifs were identified within the
200 MCMV MIEP. To analyze the function of these putative transcription factor binding sites, we
201 inserted the WT MIEP and six mutant versions (Table S1) into the luciferase reporter plasmid
202 pGL3-Basic. In the mutant MIEPs, one or all five ACGT motifs were changed to CTAG. Using
203 a luciferase reporter assay, we measured MIEP activity in WT, *Ire1* ko and *Xbp1* ko
204 fibroblasts. As shown in Fig. 7A, MIEP activity was strongly reduced in *Ire1* ko cell but was
205 not significantly altered in *Xbp1* ko cells. This result is consistent with the MCMV replication
206 defect observed in *Ire1*, but not *Xbp1* ko cells (Fig. 3B). MIEP activity was not reduced in
207 *Xbp1*/*Ire1* dko cells compared to the parental *Xbp1* ko cell (Fig. 7B), but was significantly
208 reduced in *Atf6*/*Xbp1* dko cells compared to the parental *Atf6* ko cells (Fig. 7C). Again, the
209 MIEP activities were consistent with the results of the viral replication kinetics (Figs. 5B and
210 6D). Thus, we concluded that activation of the MCMV MIEP correlated with viral replication in
211 the same cells. We also found that the activity of the MIEP had a substantially reduced
212 activity when all 5 ACGT motifs were mutated (Fig. 7A-C).
213 Next we tested whether XBP1s and ATF6(N), the active form of ATF6, can activate
214 the MCMV MIEP and whether XBP1u can repress it. To assess the contribution of
215 endogenous levels of the TFs, *Xbp1* ko, *Atf6* ko, and *Xbp1*/*Atf6* dko cells were used. In *Xbp1*
216 ko cells, MIEP activity was slightly increased by expression of XBP1s, but substantially
217 reduced by XBP1u. XBP1u also antagonized XBP1s in a dose-dependent manner (Fig. 7D).
218 A similar result was obtained in *Atf6*$^{-/-}$ cells: MIEP activity was slightly increased by
219 expression of ATF6(N), but substantially reduced by XBP1u. XBP1u also antagonized
220 ATF6(N) in a dose-dependent manner (Fig. 7E). In *Atf6*/*Xbp1* dko cell, expression of either
221 XBP1s or ATF6(N) was sufficient to increase MIEP activity substantially. XBP1u alone did

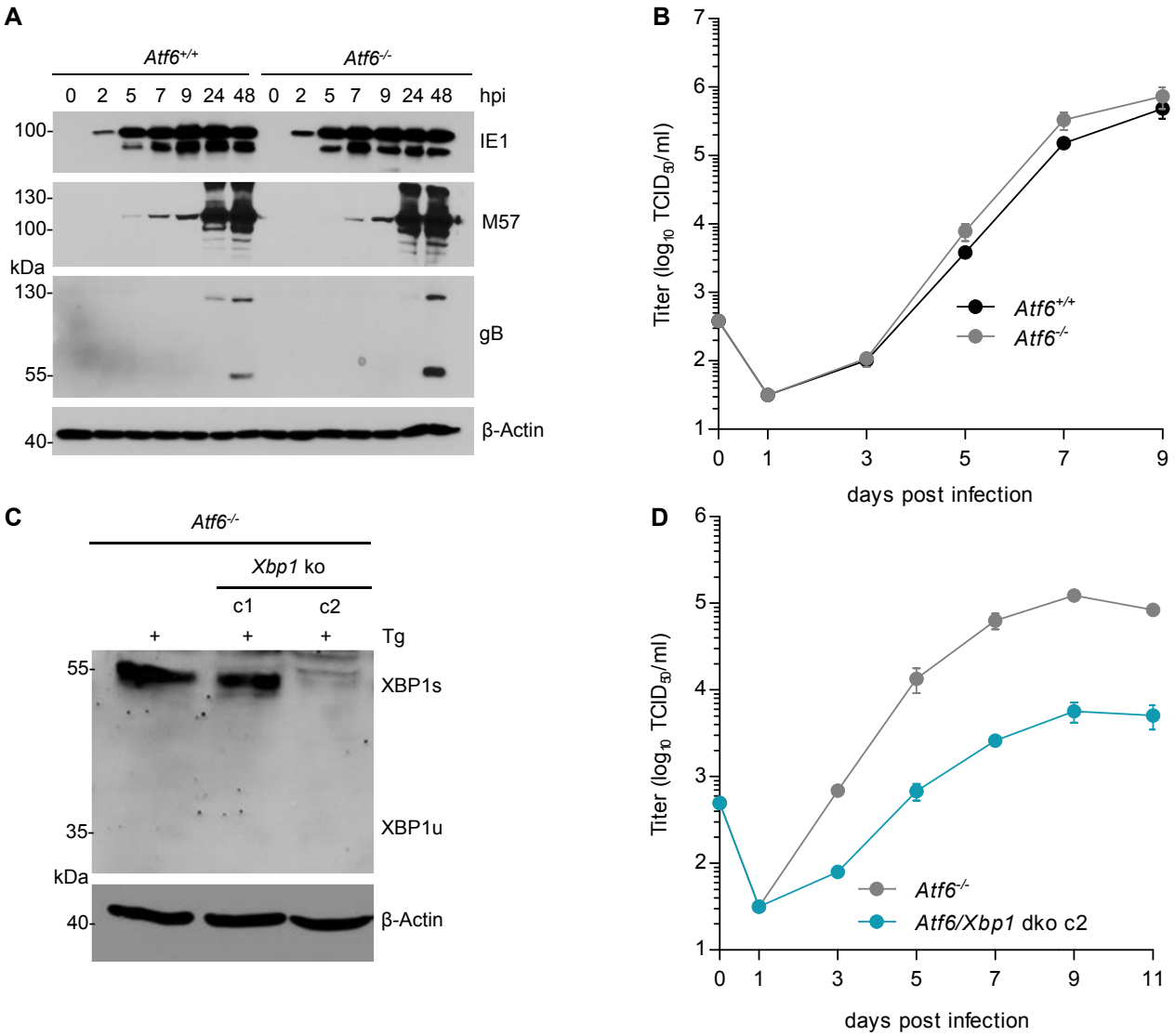

Figure 6.
MCMV replication is impaired in cells lacking *Atf6* and *Xbp1*.

A. Immunoblot analysis of viral gene expression of *Atf6*$^{+/+}$ and *Atf6*$^{-/-}$ cells infected with MCMV-GFP at an MOI of 3 $TCID_{50}$/ml. At indicated times cells were lysed and stained for the immediate-early 1 protein (IE1), the major DNA binding protein (M57; early gene) and glycoprotein B (gB; late gene) by immunoblot. β-Actin served as loading control.

B. Multistep replication kinetics. *Atf6*$^{+/+}$ and *Atf6*$^{-/-}$ cells were infected with MCMV-GFP at an MOI of 0.1 $TCID_{50}$/ml. Virus titers in the supernatants were determined by titration and are shown as means ±SEM of triplicates.

C. Knockout of *Xbp1* in *Atf6*$^{-/-}$ cells using CRISPR/Cas9 gene editing. Two single cell clones generated by two individual gRNAs (c1 and c2) were analyzed for XBP1s and XBP1u expression by immunoblot. 4h prior to harvesting, cells were stimulated with thapsigargin (Tg) to enhance XBP1 expression. The parental *Atf6*$^{-/-}$ cells are shown as control.

D. Multistep replication kinetics of *Atf6*/*Xbp1* dko cells (clone c2). MCMV infection and titration was done as described in B.

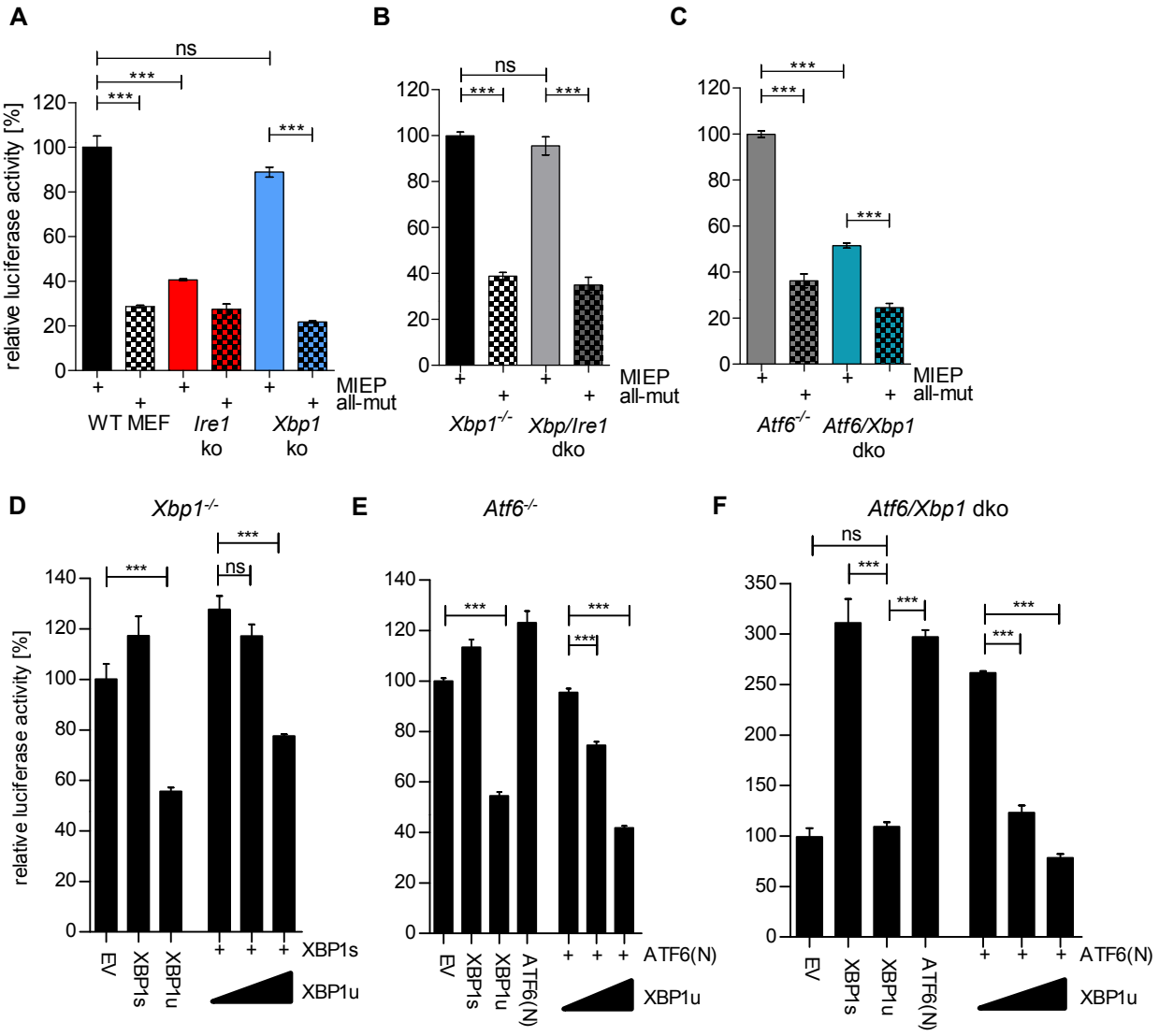

Figure 7. XBP1s and ATF6-mediated activation of the MCMV MIEP is repressed by XBP1u.

A WT MEFs, *Ire1* ko and *Xbp1* ko cells were transfected with a firefly luciferase vector containing either the WT major immediate-early promotor (MIEP) or a MIEP with 5 mutated ACGT motifs (all-mut). Renilla luciferase was expressed by co-transfection and used for normalization. Relative luciferase activities (firefly : renilla) ±SEM of 3 biological replicates are shown.

B *Xbp1*$^{-/-}$ and *Xbp1/Ire1* dko cells were transfected as in A and the relative luciferase activity was determined.

C *Atf6*$^{-/-}$ and *Atf6/Xbp1* dko cells were transfected as in A and the relative luciferase activity was determined.

D *Xbp1*$^{-/-}$ MEFs were co-transfected with firefly and renilla luciferase vectors as in A. Expression vectors for XBP1s, XBP1u, ATF6(N), or empty vector (EV) were co-transfected. Relative luciferase activities (firefly : renilla) ±SEM of 3 biological replicates are shown.

E *Atf6*$^{-/-}$ cells were transfected as in D and the relative luciferase activity was determined.

F *Atf6/Xbp1* dko cells were transfected as in A and the relative luciferase activity was determined.

222 not reduce MIEP activity in these cells, but it antagonized the activity of ATF6(N) expressed
223 by transfection (Fig. 7F). Taken together, these results suggest that both, XBP1s and
224 ATF6(N), can activate the MCMV MIEP in a largely redundant fashion, and that XBP1u
225 represses the activity of both, XBP1s and ATF6(N).
226
227 **Motif 4 is necessary and sufficient for MIEP activation by XBP1s and ATF6(N).**
228 As a first step to determine, which of the five ACGT motifs function as XBP1s and/or
229 ATF6(N) binding sites for promoter activation, we measured the binding of these TFs to
230 portions of the MIEP by using a DNA-protein interaction ELISA (DPI-ELISA, (Brand et al,
231 2010; Underwood et al, 2013). Microtiter plates were coated with double-stranded
232 oligonucleotides encoding three copies (27 nucleotides each) of a putative binding motif with
233 adjacent sequences on either side (Table S3). A known XBP1 binding motif of the ERdj4
234 promoter (Kanemoto et al, 2005) served as positive control and a sequence of the SV40
235 origin of replication as negative control. The oligonucleotides were incubated with HA-tagged
236 XBP1s, XBP1u, or ATF6(N) (Fig. 8A), and DNA binding was quantified by ELISA. Mutated
237 TFs lacking the DNA-binding domain (ΔDBD) served as negative controls. In this DPI-ELISA,
238 XBP1s and XBP1u showed the strongest interaction with motifs 3 and 4, whereas ATF6(N)
239 interacted with motifs 2 and 4 (Fig. 8B).
240 Next we used the luciferase reporter assay to test which of the five motifs was
241 required for MIEP activation by XBP1s and ATF6(N). We used five mutants MIEPs having
242 one of the ACGT motifs changed to CTAG. These reporter plasmids were transfected into
243 *Atf6*/*Xbp1* dko cells, together with expression plasmids for XBP1s, XBP1u, and ATF6(N). As
244 shown in Fig. 9A, XBP1s or ATF6(N) expression increased the activity of all MIEP constructs
245 except MIEP-4mut and MIEP-all-mut, indicating that ACGT motif 4 is necessary for MIEP
246 activation by XBP1s and ATF6(N).
247 Finally, we tested whether motif 4 was also sufficient for MIEP activation by XBP1s
248 and ATF6(N). Motif 4 was restored in MIEP-all-mut to generate a MIEP containing only
249 ACGT motif 4 (MIEP-4only, Table S1). Indeed, MIEP-4only was inducible by XBP1s and
250 ATF6(N) (Fig. 9B), suggesting that motif 4 is sufficient to confer MIEP responsiveness to
251 XBP1s and ATF6.
252 Taken together, the results of this study show that MCMV transiently activates the
253 IRE1-XBP1 signaling pathway in the early phase of infection in order to relieve XBP1u-
254 mediated repression of viral gene expression and replication. The MCMV major immediate-
255 early promoter requires XBP1s or ATF6(N) for full activation, and XBP1u represses the
256 activity of both TFs. Thus, XBP1u acts as a key repressor of two UPR pathways, the IRE1-
257 XBP1 and the ATF6 pathways, which have overlapping and redundant functions.
258

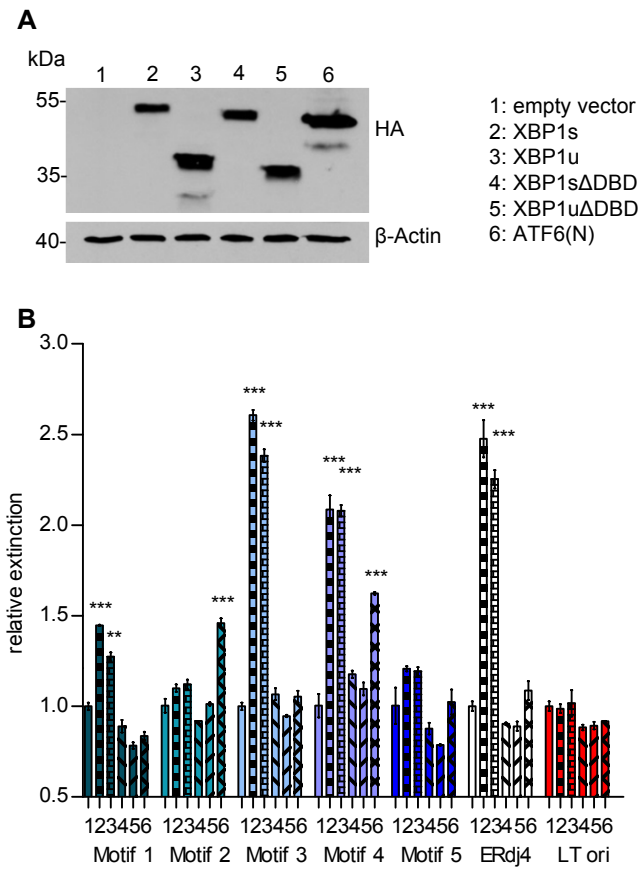

Figure 8. Transcription factor binding the MIE promotor

A. HEK 293A cells were transfected with expression vectors encoding HA-tagged WT or mutant XBP1 and ATF6(N) transcription factors. Nuclear extracts were obtained, and transcription factor expression was verified by immunoblot analysis.

B. Microtiter plates coated with dsDNA oligonucleotides containing XBP1 core binding motifs from the MCMV major immediate-early promoter, the ERdj4 promoter (positive control) or an unrelated sequence from the SV40 origin of replication (negative control). Wells were incubated with nuclear extracts 1 to 6 shown in A, and transcription factor binding was measured by DPI-ELISA, and values were normalized to extract 1 (empty vector). Means ±SEM of triplicates are shown. **, $p<0.01$; ***, $p<0.001$.

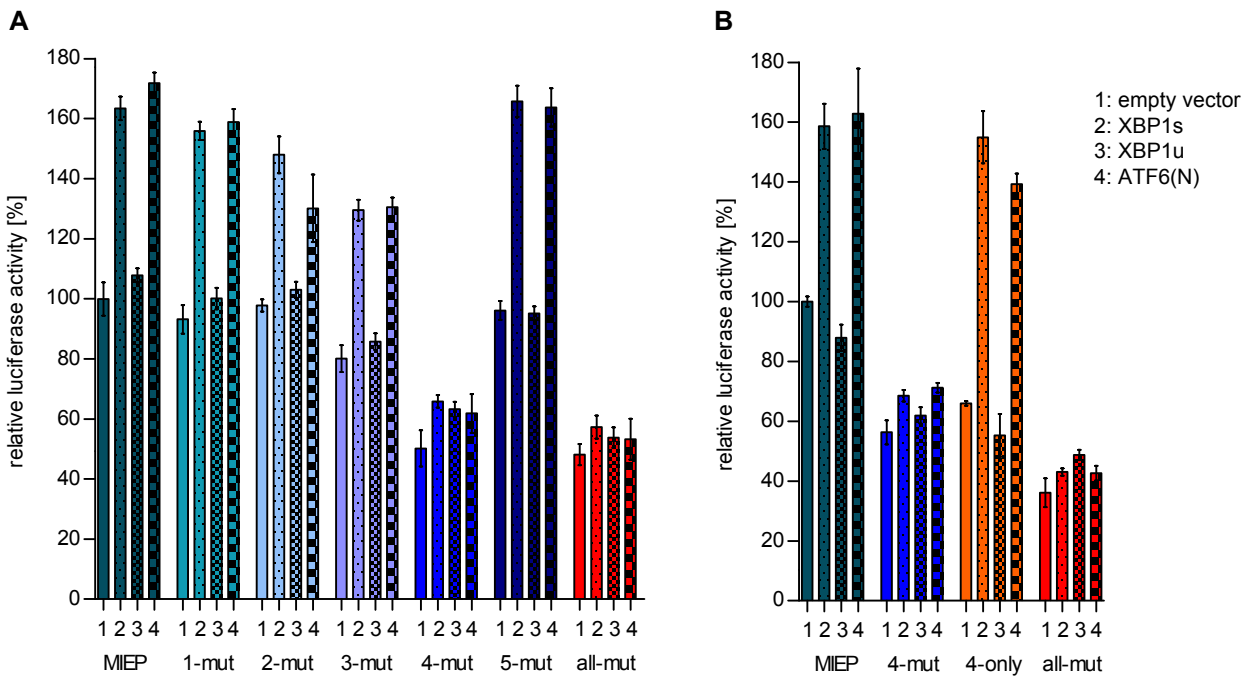

Figure 9. Motif 4 is necessary and sufficient for MIEP activation by XBP1s and ATF6(N).

A *Atf6/Xbp1* dko MEFs cells were transfected with a firefly luciferase vector containing either the WT major immediate-early promotor (MIEP) or a MIEP with 1 or all ACGT motifs mutated. Expression vectors for XBP1a, XBP1u, ATF6(N), or empty vector (EV) were co-transfected. Renilla luciferase was expressed by co-transfection and used for normalization. Relative luciferase activities (firefly : renilla) ±SEM of 3 biological replicates are shown.

B *Atf6/Xbp1* dko MEF cells were transfected and analyzed as in A. In addition, a MIEP vector with all ACGT motifs mutated except motif 4 (4-only) was included.

Discussion

This study shows how MCMV harnesses UPR signaling to regulate its own life cycle. The viral MIEP, the key promotor of the lytic replication cycle, contains five ACGT motifs, of which motif 4 is most important for MIEP activation by XBP1s or ATF6(N) (Fig. 9). The fact that MIEP activity and viral replication are virtually unaffected in the absence of either XBP1 or ATF6 but are massively reduced in the absence of both, strongly suggests that the two UPR TFs have redundant roles in the activation of the MIEP. The most important finding, however, is the dominant role of XBP1u as a repressor of viral gene expression and replication. When IRE1 is absent or its RNase activity is blocked, XBP1u dominates and prevents MIEP activation by XBP1s and ATF6(N). Thus, the transient activation of IRE1 during the early phase of MCMV infection serves the virus by increasing XBP1s and decreasing XBP1u expression, thereby relieving XPB1u-mediated repression.

How exactly XBP1u antagonizes XBP1s and ATF6(N)-mediated promoter activation, remains to be determined. Two possible mechanisms may be involved: XBP1u could interact with XBP1s and ATF6(N) and target them for proteasomal degradation as previously reported (Yoshida et al, 2006; Yoshida et al, 2009). Additionally, XBP1u could bind directly to DNA and inhibit promoter activation by XBP1s and ATF6(N). Indeed, we show that XBP1u is fully capable of binding to the same DNA sequences that XBP1s binds to (Fig. 8). Moreover, a truncated XBP1 protein, XBP1stop, which lacks the C-terminal destabilizing domain of XBP1u, had a similar repressive effect as XBP1u (Fig 5D) indicating that destabilization is not required for repression.

Ever since its discovery, the importance of XBP1u has been the subject of controversy. In yeast, the unspliced mRNA of HAC1, the yeast homolog of XBP1, is posttranscrptionally silenced, and a protein product of the unspliced HAC1 mRNA has not been detected (Ruegsegger et al, 2001). In mammalian cells, the XBP1u protein is readily detectable, but XBP1u has a short half-life (Navon et al, 2010; Tirosh et al, 2006). This has led to the conclusion that XBP1u is of minor importance and its function restricted to fine-tuning of the UPR (Byrd & Brewer, 2012). Hence, many review articles on the UPR barely mention XBP1u. On the other hand, XBP1u has been shown to dimerize with XBP1s and ATF6(N) and destabilize them (Yoshida et al, 2006; Yoshida et al, 2009), suggesting a more important regulatory role. However, the physiological relevance of these findings has been called into question by some scientists because the findings were made in cells overexpressing XBP1u. The results of our study show that XBP1u plays a very important role as a repressor of XBP1s and ATF6(N)-mediated activation of the MCMV MIEP, which results in a massively (~100-fold) reduced production of progeny virus (Figs. 2, 3B, and 5D). In IRE1 ko cells, the XBP1 transcript is expressed from its endogenous promoter, not from a strong heterologous promoter. Thus, the observed effects cannot be dismissed as overexpression

296 artifacts. Moreover, the fact that MCMV replication is massively reduced in IRE1 ko cells
297 (Figs. 2 and 3B), but not in IRE1/XBP1 dko cells (Fig. 5B), demonstrates that XBP1u
298 expression rather than the absence RIDD is responsible for the observed effect. Hence, the
299 data of our study suggest that XBP1u plays an unexpectedly important role as a repressor, at
300 least under the conditions of viral infection. Whether XBP1u can repress expression of
301 cellular genes in a similar fashion is an important question that needs to be answered in
302 future studies.
303 XBP1 binding sites have also been identified in immediate-early gene promoters of
304 the γ-herpesviruses Epstein-Barr virus, Kaposi's sarcoma-associated herpesvirus, and
305 murine gammaherpesvirus 68 (MHV-68), suggesting a potential role for XBP1s in
306 transactivating these promoters during reactivation from latency (Bhende et al, 2007; Matar
307 et al, 2014; Sun & Thorley-Lawson, 2007; Wilson et al, 2007; Yu et al, 2007). However, one
308 study demonstrated that XBP1 was not required for MHV-68 reactivation in B cells (Matar et
309 al, 2014). The authors of the study speculated that the apparent independence of MHV-68
310 reactivation from XBP1 expression in B cells might reflect redundancy among CREB/ATF
311 family TFs. In light of our data showing a redundancy of XBP1s and ATF6(N) in the activation
312 of the MCMV MIEP, this speculation may well be correct. Conversely, it would be interesting
313 to know whether XBP1 and ATF6 also regulate MCMV reactivation from latency.
314 Unfortunately, this obvious question is difficult to address as there is no manageable
315 experimental system for MCMV latency and reactivation. Nonetheless, it appears likely that β
316 and γ-herpesviruses harness UPR TFs in a similar fashion to regulate their life cycle.
317
318
319 **Materials and Methods**
320 **Cells and viruses**
321 The following immortalized fibroblast lines were used: wildtype MEFs (Manzl et al, 2009),
322 10.1 cells (Harvey & Levine, 1991), *Xbp1*$^{-/-}$ MEFs (Reimold et al, 2000), Primary *Atf6*$^{+/+}$ and
323 *Atf6*$^{-/-}$ MEFs (Wu et al, 2007) were kindly provided by D. Thomas Rutkowski (University of
324 Iowa, USA). They were immortalized by transduction with a retroviral vector encoding SV40
325 large T antigen (pBABE-zeo largeTcDNA, Addgene). The *Atf6*$^{+/+}$ vs. *Atf6*$^{-/-}$ state was verified
326 by PCR as described (Wu et al, 2007). TetON-IRE1-GFP MEFs were obtained by
327 reconstituting *Ire1*$^{-/-}$ MEFs with GFP-tagged murine IRE1 under control of a 'tight' Tet-
328 responsive element (Clontech) essentially as described (Bakunts et al, 2017; Cohen et al,
329 2017). The GFP tag was introduced into the juxtamembrane cytosolic linker domain of IRE1,
330 where such tagging had been shown before to not interfere with function of human IRE1 (Li
331 et al, 2010). All cells were grown under standard conditions in Dulbecco´s modified Eagle´s

332 medium supplemented with 10% fetal calf serum or 10% fetal calf serum tetracycline-free,
333 100 IU/ml penicillin and 100 µg/ml streptomycin (Sigma).
334 MCMV-GFP (Brune et al, 2001) was propagated and titrated on 10.1 fibroblasts. Viral
335 titers were determined by using the median tissue culture infective dose ($TCID_{50}$) method.
336 Virus was inactivated by 254-nm-wavelength UV irradiation with 1 J/cm^2 for 30 s using a UV
337 cross-linker (HL-2000 HybriLinker; UVP).
338
339 **Plasmids and transfection**
340 XBP1-wt and XBP1-unsplicable cDNAs (Tirosh et al, 2006) were cloned in pcDNA3. The
341 XBP1-wt vector was used to generate by PCR an XBP1stop mutant consisting of only the N-
342 terminal domain of XBP1. The XBP1s cDNA was generated by isolating RNA from MEFs
343 stimulated with tunicamycin (Sigma), reverse transcription, and PCR amplification. To
344 generate XBP1-unsplicable and XBP1-spliced plasmids lacking the DNA-binding domain
345 (ΔDBD) the complete DBD was replaced by an alternative NLS sequence as previously
346 described (Zhou et al, 2011). Transcripts of XBP1 proteins were HA-tagged by PCR
347 amplification and subcloned in pMSCVpuro (Clonetech), a retroviral vector plasmid. Similarly,
348 mIRE1-wt was PCR-amplified (without a myc tag) from pcDNA3-mIRE1-3xmyc (Stahl et al,
349 2013) and subcloned in pMSCVhyg (Clontech) using BglII and HpaI sites. The K907A
350 mutation was introduced by QuikChange site-directed mutagenesis (Stratagene). Transient
351 transfection was done using GenJet (SignaGen) or polyethylenimine (Sigma).
352
353 **Retroviral transduction and CRISPR/Cas9 gene editing**
354 Retrovirus production using the Phoenix packaging cell line and transduction of target cells
355 was done as described (Swift et al, 2001). Cells transduced with MSCVpuro and MSCVhyg
356 vectors were selected with 1.5 µg/ml puromycin (Sigma) or 50 µg/ml hygromycin B (Roth),
357 respectively.
358 Guide RNAs (Table S2) for genes of interest were designed using the online tool E-
359 CRISP (http://www.e-crisp.org/E-CRISP/designcrispr.html) and inserted into the lentiviral
360 vector pSicoR-CRISPR-puroR (kindly provided by R. J. Lebbink, University Medical Center
361 Utrecht, Netherlands). Lentiviruses were produced in 293T cells using standard third-
362 generation packaging vectors as described (van Diemen et al, 2016). Lentiviruses were used
363 to transduce MEFs in the presence of polybrene (5 µg/ml). Cells were selected with 1.5 µg/ml
364 puromycin and single cell clones were obtained by limiting dilution.
365
366

367 **Immunoblot analysis**

368 Whole cell lysates were obtained by lysing cells in RIPA buffer supplemented with a
369 cOmplete™, Mini protease inhibitor cocktail (Roche). XBP1s, XBP1u, and ATF6(N) were
370 extracted from cells treated with thapsigargin (Sigma) using a nuclear extraction protocol
371 (Stahl et al, 2013). Insoluble material was removed by centrifugation. Protein concentrations
372 were measured using a BCA assay (company). Equal protein amounts were boiled in sample
373 buffer and subjected to SDS-PAGE and semi-dry blotting onto nitrocellulose membranes. For
374 immunodetection, antibodies against the following epitopes were used: HA (16B12,
375 BioLegend), β-actin (AC-74, Sigma), XBP1 (M-186, Santa Cruz), IRE1 (14C10, Cell
376 Signaling), TRAF2 (Cell Signaling), and GFP (Roche). Antibodies against MCMV IE1
377 (CROMA101), M57, and M55/gB (SN1.07) were provided by Stipan Jonjic (University of
378 Rijeka, Croatia). Secondary antibodies coupled to horseradish peroxidase (HRP) were
379 purchased from Dako.

380

381 **RNA isolation and quantitative PCR**

382 Total RNA was isolated from MEFs using an innuPREP RNA Mini Kit (Analytik-Jena).
383 Reverse transcription and cDNA synthesis was carried out with 2 µg RNA using 200 U
384 RevertAid H Minus Reverse Transcriptase, 100 pmol Oligo$(dT)_{18}$, and 20 U RNase inhibitor
385 (Thermo Fisher Scientific). Quantitative real-time PCR reactions employing SYBR Green
386 were run in an 7900HT Fast Real-Time PCR System (Applied Biosystems). The following
387 primers were used: 5′-GAGTCCGCAGCAGGTG-3′ and 5′-GTGTCAGAGTCCATGGGA-3′ for
388 *Xbp1s*, 5′-GTGTCAGAGTCCATGGGA-3′ and 5′-GTGTCAGAGTCCATGGGA-3′ for X*bp1u,*
389 *and* 5′-CCCACTCTTCCACCTTCGATG-3′ and 5′-GTCCACCACCCTGTTGCTGTAG-3′ for
390 *Gapdh*. Reactions were performed under the following conditions: 45 cycles of 3 sec at 95°C
391 and 30 sec at 60°C. Three replicates were analyzed for each condition, and the relative
392 amounts of mRNAs were calculated from the comparative threshold cycle (Ct) values by
393 using *Gapdh* as reference.

394

395 **Replication kinetics**

396 Cells were seeded in 6-well plates and infected by an MOI of 3 or 0.1 for single or multi-step
397 replication kinetics, respectively. Six hpi the medium was exchanged to remove the
398 inoculum. Supernatant samples were harvested at different times post infection, and viral
399 titers were determined on 10.1 fibroblasts using the $TCID_{50}$ method.

400

401 **MIE promotor activity assay**

402 The firefly luciferase reporter vector pGL3-Basic, the renilla luciferase control vector
403 pGL4.73, and the Dual-Glo Luciferase assay system were purchased from Promega. WT

404 and mutant versions of the MCMV MIE promotor (Table S1) were synthesized by Integrated
405 DNA Technologies and cloned in pGL3-Basic. Cells were transfect in 6-well dishes using
406 GenJet with pGL3-MIEP (0.5 µg), pGL4.73 (0.05 µg) and transcription factor expression
407 plasmids. The total amount of DNA was kept constant at 3 µg by filling up with empty
408 pcDNA3 vector. On the following day, the medium was exchanged and cells were incubated
409 for another 24 h. Cells were harvested in lysis buffer and luciferase activity was measured
410 using a Dual-Glo Luciferase assay and a luminescence plate reader (FLUOstar-Omega,
411 BMG Labtech). Firefly and Renilla luciferase activities were evaluated for each sample. At
412 least 3 biological replicates were used for each condition.
413
414 **DNA-Protein Interaction ELISA (DPI-ELISA)**
415 The DPI-ELISA was performed essentially as described in detail elsewhere (Brand et al,
416 2010; Underwood et al, 2013). Terminally biotinylated dsDNA oligonucleotides containing 3
417 copies of putative TF binding sites (Table S3) were purchased from Eurofins.
418 Oligonucleotides were adsorbed to streptavidin-coated 96-well microtiter plates and
419 incubated with nuclear extracts (10 µg protein) from transfected HEK 293A cells expressing
420 the HA-tagged XBP1 or ATF6(N) proteins. Nuclear extracts were obtained as described
421 (Stahl et al, 2013). TF binding to DNA was quantified by ELISA using an anti-HA antibody, an
422 HRP-coupled secondary antibody, and an ABTS substrate (Roche). Absorbance at 405 nm
423 wavelength was measured using a FLUOstar-Omega plate reader. At least 3 biological
424 replicates were used for each condition.
425
426 ## Acknowledgments
427 We thank D. Thomas Rutkowski for providing *Atf6*$^{-/-}$ MEFs and Svenja Siebels for helpful
428 advice on the DPI-ELISA. This study was supported by the Deutsche
429 Forschungsgemeinschaft (BR 1730/6-1 to WB), the EU Horizon 2020 Marie Sklodowska-
430 Curie ITN-TREATMENT (Grant 721236 to BT), the German-Israeli Foundation (Grant I-1471-
431 414.13/2018 to BT), and Giovanni Armenise-Harvard Foundation (Career Development
432 Award to EvA).
433
434 ## Author contributions
435 Conceptualization, FH, BT, WB; Methodology, FH, EvA; Investigation, FH; Writing—Original
436 Draft, FH, WB; Writing—Review & Editing, FH, BT, WB; Funding Acquisition, WB;
437 Resources, EvA, BT; Supervision, WB.
438
439 ## Conflict of interest
440 The authors declare that they have no conflict of interest.

441

442

443 **References**

444 Alwine JC (2008) Modulation of host cell stress responses by human cytomegalovirus. *Curr*
445 *Top Microbiol Immunol* **325:** 263-279

446
447 Bakunts A, Orsi A, Vitale M, Cattaneo A, Lari F, Tade L, Sitia R, Raimondi A, Bachi A, van
448 Anken E (2017) Ratiometric sensing of BiP-client versus BiP levels by the unfolded protein
449 response determines its signaling amplitude. *Elife* **6**

450
451 Bhende PM, Dickerson SJ, Sun X, Feng WH, Kenney SC (2007) X-box-binding protein 1
452 activates lytic Epstein-Barr virus gene expression in combination with protein kinase D. *J*
453 *Virol* **81:** 7363-7370

454
455 Brand LH, Kirchler T, Hummel S, Chaban C, Wanke D (2010) DPI-ELISA: a fast and
456 versatile method to specify the binding of plant transcription factors to DNA in vitro. *Plant*
457 *methods* **6:** 25

458
459 Brune W, Ménard C, Heesemann J, Koszinowski UH (2001) A ribonucleotide reductase
460 homolog of cytomegalovirus and endothelial cell tropism. *Science* **291:** 303-305

461
462 Buchkovich NJ, Maguire TG, Yu Y, Paton AW, Paton JC, Alwine JC (2008) Human
463 cytomegalovirus specifically controls the levels of the endoplasmic reticulum chaperone
464 BiP/GRP78, which is required for virion assembly. *J Virol* **82:** 31-39

465
466 Buchkovich NJ, Yu Y, Pierciey FJ, Jr., Alwine JC (2010) Human cytomegalovirus induces the
467 endoplasmic reticulum chaperone BiP through increased transcription and activation of
468 translation by using the BiP internal ribosome entry site. *J Virol* **84:** 11479-11486

469
470 Byrd AE, Brewer JW (2012) Intricately Regulated: A Cellular Toolbox for Fine-Tuning XBP1
471 Expression and Activity. *Cells* **1:** 738-753

472
473 Calfon M, Zeng H, Urano F, Till JH, Hubbard SR, Harding HP, Clark SG, Ron D (2002) IRE1
474 couples endoplasmic reticulum load to secretory capacity by processing the XBP-1 mRNA.
475 *Nature* **415:** 92-96

476
477 Christianson JC, Ye Y (2014) Cleaning up in the endoplasmic reticulum: ubiquitin in charge.
478 *Nature structural & molecular biology* **21:** 325-335

479
480 Cohen N, Breker M, Bakunts A, Pesek K, Chas A, Argemi J, Orsi A, Gal L, Chuartzman S,
481 Wigelman Y, Jonas F, Walter P, Ernst R, Aragon T, van Anken E, Schuldiner M (2017) Iron
482 affects Ire1 clustering propensity and the amplitude of endoplasmic reticulum stress
483 signaling. *J Cell Sci* **130:** 3222-3233

484

485 Dolan A, Cunningham C, Hector RD, Hassan-Walker AF, Lee L, Addison C, Dargan DJ,
486 McGeoch DJ, Gatherer D, Emery VC, Griffiths PD, Sinzger C, McSharry BP, Wilkinson GW,
487 Davison AJ (2004) Genetic content of wild-type human cytomegalovirus. *J Gen Virol* **85:**
488 1301-1312

489
490 Drori A, Messerle M, Brune W, Tirosh B (2014) Lack of XBP-1 impedes murine
491 cytomegalovirus gene expression. *PLoS One* **9:** e110942

492
493 Harvey DM, Levine AJ (1991) p53 alteration is a common event in the spontaneous
494 immortalization of primary BALB/c murine embryo fibroblasts. *Genes Dev* **5:** 2375-2385

495
496 Isler JA, Skalet AH, Alwine JC (2005) Human cytomegalovirus infection activates and
497 regulates the unfolded protein response. *J Virol* **79:** 6890-6899

498
499 Kanemoto S, Kondo S, Ogata M, Murakami T, Urano F, Imaizumi K (2005) XBP1 activates
500 the transcription of its target genes via an ACGT core sequence under ER stress. *Biochem*
501 *Biophys Res Commun* **331:** 1146-1153

502
503 Lacaze P, Forster T, Ross A, Kerr LE, Salvo-Chirnside E, Lisnic VJ, Lopez-Campos GH,
504 Garcia-Ramirez JJ, Messerle M, Trgovcich J, Angulo A, Ghazal P (2011) Temporal profiling
505 of the coding and noncoding murine cytomegalovirus transcriptomes. *J Virol* **85:** 6065-6076

506
507 Lee K, Tirasophon W, Shen X, Michalak M, Prywes R, Okada T, Yoshida H, Mori K,
508 Kaufman RJ (2002) IRE1-mediated unconventional mRNA splicing and S2P-mediated ATF6
509 cleavage merge to regulate XBP1 in signaling the unfolded protein response. *Genes Dev* **16:**
510 452-466

511
512 Li H, Korennykh AV, Behrman SL, Walter P (2010) Mammalian endoplasmic reticulum stress
513 sensor IRE1 signals by dynamic clustering. *Proc Natl Acad Sci U S A* **107:** 16113-16118

514
515 Manzl C, Krumschnabel G, Bock F, Sohm B, Labi V, Baumgartner F, Logette E, Tschopp J,
516 Villunger A (2009) Caspase-2 activation in the absence of PIDDosome formation. *J Cell Biol*
517 **185:** 291-303

518
519 Marcinowski L, Lidschreiber M, Windhager L, Rieder M, Bosse JB, Radle B, Bonfert T, Gyory
520 I, de Graaf M, Prazeres da Costa O, Rosenstiel P, Friedel CC, Zimmer R, Ruzsics Z, Dolken
521 L (2012) Real-time transcriptional profiling of cellular and viral gene expression during lytic
522 cytomegalovirus infection. *PLoS Pathog* **8:** e1002908

523
524 Matar CG, Rangaswamy US, Wakeman BS, Iwakoshi N, Speck SH (2014) Murine
525 gammaherpesvirus 68 reactivation from B cells requires IRF4 but not XBP-1. *J Virol* **88:**
526 11600-11610

527
528 Maurel M, Chevet E, Tavernier J, Gerlo S (2014) Getting RIDD of RNA: IRE1 in cell fate
529 regulation. *Trends Biochem Sci* **39:** 245-254

530

531 Mocarski ES, Jr. (2002) Immunomodulation by cytomegaloviruses: manipulative strategies
532 beyond evasion. *Trends Microbiol* **10:** 332-339

533
534 Moore K, Hollien J (2015) Ire1-mediated decay in mammalian cells relies on mRNA
535 sequence, structure, and translational status. *Mol Biol Cell* **26:** 2873-2884

536
537 Navon A, Gatushkin A, Zelcbuch L, Shteingart S, Farago M, Hadar R, Tirosh B (2010) Direct
538 proteasome binding and subsequent degradation of unspliced XBP-1 prevent its intracellular
539 aggregation. *FEBS Lett* **584:** 67-73

540
541 Novoa I, Zeng H, Harding HP, Ron D (2001) Feedback inhibition of the unfolded protein
542 response by GADD34-mediated dephosphorylation of eIF2alpha. *J Cell Biol* **153:** 1011-1022

543
544 Qian Z, Xuan B, Chapa TJ, Gualberto N, Yu D (2012) Murine cytomegalovirus targets
545 transcription factor ATF4 to exploit the unfolded-protein response. *J Virol* **86:** 6712-6723

546
547 Reimold AM, Etkin A, Clauss I, Perkins A, Friend DS, Zhang J, Horton HF, Scott A, Orkin SH,
548 Byrne MC, Grusby MJ, Glimcher LH (2000) An essential role in liver development for
549 transcription factor XBP-1. *Genes Dev* **14:** 152-157

550
551 Ruegsegger U, Leber JH, Walter P (2001) Block of HAC1 mRNA translation by long-range
552 base pairing is released by cytoplasmic splicing upon induction of the unfolded protein
553 response. *Cell* **107:** 103-114

554
555 Smith MH, Ploegh HL, Weissman JS (2011) Road to ruin: targeting proteins for degradation
556 in the endoplasmic reticulum. *Science* **334:** 1086-1090

557
558 Stahl S, Burkhart JM, Hinte F, Tirosh B, Mohr H, Zahedi RP, Sickmann A, Ruzsics Z, Budt M,
559 Brune W (2013) Cytomegalovirus downregulates IRE1 to repress the unfolded protein
560 response. *PLoS Pathog* **9:** e1003544

561
562 Stern-Ginossar N, Weisburd B, Michalski A, Le VT, Hein MY, Huang SX, Ma M, Shen B,
563 Qian SB, Hengel H, Mann M, Ingolia NT, Weissman JS (2012) Decoding human
564 cytomegalovirus. *Science* **338:** 1088-1093

565
566 Sun CC, Thorley-Lawson DA (2007) Plasma cell-specific transcription factor XBP-1s binds to
567 and transactivates the Epstein-Barr virus BZLF1 promoter. *J Virol* **81:** 13566-13577

568
569 Swift S, Lorens J, Achacoso P, Nolan GP (2001) Rapid production of retroviruses for efficient
570 gene delivery to mammalian cells using 293T cell-based systems. *Curr Protoc Immunol*
571 **Chapter 10:** Unit 10 17C

572
573 Tirasophon W, Lee K, Callaghan B, Welihinda A, Kaufman RJ (2000) The endoribonuclease
574 activity of mammalian IRE1 autoregulates its mRNA and is required for the unfolded protein
575 response. *Genes Dev* **14:** 2725-2736

576
577 Tirosh B, Iwakoshi NN, Glimcher LH, Ploegh HL (2006) Rapid turnover of unspliced Xbp-1 as
578 a factor that modulates the unfolded protein response. *J Biol Chem* **281:** 5852-5860

579
580 Underwood KF, Mochin MT, Brusgard JL, Choe M, Gnatt A, Passaniti A (2013) A quantitative
581 assay to study protein:DNA interactions, discover transcriptional regulators of gene
582 expression, and identify novel anti-tumor agents. *Journal of visualized experiments : JoVE*

583
584 Urano F, Wang X, Bertolotti A, Zhang Y, Chung P, Harding HP, Ron D (2000) Coupling of
585 stress in the ER to activation of JNK protein kinases by transmembrane protein kinase IRE1.
586 *Science* **287:** 664-666

587
588 van Diemen FR, Kruse EM, Hooykaas MJ, Bruggeling CE, Schurch AC, van Ham PM, Imhof
589 SM, Nijhuis M, Wiertz EJ, Lebbink RJ (2016) CRISPR/Cas9-Mediated Genome Editing of
590 Herpesviruses Limits Productive and Latent Infections. *PLoS Pathog* **12:** e1005701

591
592 Walter P, Ron D (2011) The unfolded protein response: from stress pathway to homeostatic
593 regulation. *Science* **334:** 1081-1086

594
595 Wang Y, Shen J, Arenzana N, Tirasophon W, Kaufman RJ, Prywes R (2000) Activation of
596 ATF6 and an ATF6 DNA binding site by the endoplasmic reticulum stress response. *J Biol*
597 *Chem* **275:** 27013-27020

598
599 Wilson SJ, Tsao EH, Webb BL, Ye H, Dalton-Griffin L, Tsantoulas C, Gale CV, Du MQ,
600 Whitehouse A, Kellam P (2007) X box binding protein XBP-1s transactivates the Kaposi's
601 sarcoma-associated herpesvirus (KSHV) ORF50 promoter, linking plasma cell differentiation
602 to KSHV reactivation from latency. *J Virol* **81:** 13578-13586

603
604 Wu J, Rutkowski DT, Dubois M, Swathirajan J, Saunders T, Wang J, Song B, Yau GD,
605 Kaufman RJ (2007) ATF6alpha optimizes long-term endoplasmic reticulum function to
606 protect cells from chronic stress. *Dev Cell* **13:** 351-364

607
608 Yoshida H, Haze K, Yanagi H, Yura T, Mori K (1998) Identification of the cis-acting
609 endoplasmic reticulum stress response element responsible for transcriptional induction of
610 mammalian glucose-regulated proteins. Involvement of basic leucine zipper transcription
611 factors. *J Biol Chem* **273:** 33741-33749

612
613 Yoshida H, Matsui T, Yamamoto A, Okada T, Mori K (2001) XBP1 mRNA is induced by
614 ATF6 and spliced by IRE1 in response to ER stress to produce a highly active transcription
615 factor. *Cell* **107:** 881-891

616
617 Yoshida H, Oku M, Suzuki M, Mori K (2006) pXBP1(U) encoded in XBP1 pre-mRNA
618 negatively regulates unfolded protein response activator pXBP1(S) in mammalian ER stress
619 response. *J Cell Biol* **172:** 565-575

620

621 Yoshida H, Uemura A, Mori K (2009) pXBP1(U), a negative regulator of the unfolded protein
622 response activator pXBP1(S), targets ATF6 but not ATF4 in proteasome-mediated
623 degradation. *Cell structure and function* **34:** 1-10

624

625 Yu F, Feng J, Harada JN, Chanda SK, Kenney SC, Sun R (2007) B cell terminal
626 differentiation factor XBP-1 induces reactivation of Kaposi's sarcoma-associated herpesvirus.
627 *FEBS Lett* **581:** 3485-3488

628

629 Yu Y, Pierciey FJ, Jr., Maguire TG, Alwine JC (2013) PKR-like endoplasmic reticulum kinase
630 is necessary for lipogenic activation during HCMV infection. *PLoS Pathog* **9:** e1003266

631

632 Zhang L, Wang A (2012) Virus-induced ER stress and the unfolded protein response. *Front*
633 *Plant Sci* **3:** 293

634

635 Zhao Y, Li X, Ma K, Yang J, Zhou J, Fu W, Wei F, Wang L, Zhu WG (2013) The axis of
636 MAPK1/3-XBP1u-FOXO1 controls autophagic dynamics in cancer cells. *Autophagy* **9:** 794-
637 796

638

639 Zhou Y, Lee J, Reno CM, Sun C, Park SW, Chung J, Fisher SJ, White MF, Biddinger SB,
640 Ozcan U (2011) Regulation of glucose homeostasis through a XBP-1-FoxO1 interaction. *Nat*
641 *Med* **17:** 356-365

642

643

644